Multiple ER–Golgi SNARE transmembrane domains are dispensable for trafficking but required for SNARE recycling

Li Chen, Martin S. Y. Lau, and David K. Banfield*
Division of Life Science, Hong Kong University of Science and Technology, Kowloon, Hong Kong, China

ABSTRACT **The formation of soluble *N*-ethylmaleimide–sensitive factor attachment protein receptor (SNARE) complexes between opposing membranes is an essential prerequisite for fusion between vesicles and their target compartments. The composition and length of a SNARE's transmembrane domain (TMD) is also an indicator for their steady-state distribution in cells. The evolutionary conservation of the SNARE TMD, together with the strict requirement of this feature for membrane fusion in biochemical studies, implies that the TMD represents an essential protein module. Paradoxically, we find that for several essential ER- and Golgi-localized SNAREs, a TMD is unnecessary. Moreover, in the absence of a covalent membrane tether, such SNAREs can still support ER–Golgi vesicle transport and recapitulate established genetic interactions. Transport anomalies appear to be restricted to retrograde trafficking, but these defects are overcome by the attachment of a C-terminal lipid anchor to the SNARE. We conclude that the TMD functions principally to support the recycling of Qb-, Qc-, and R-SNAREs and, in so doing, retrograde transport.**

Monitoring Editor
Akihiko Nakano
RIKEN

Received: May 9, 2016
Revised: Jun 27, 2016
Accepted: Jun 29, 2016

INTRODUCTION

Distinct sets of soluble *N*-ethylmaleimide–sensitive factor attachment protein receptors (SNAREs) are required for the terminal step of a variety of membrane fusion events in cells (Chen and Scheller, 2001; Jahn and Scheller, 2006). SNAREs are typically type II integral membrane proteins that use a signal recognition–particle independent mechanism for insertion into the endoplasmic reticulum (ER; Kutay *et al.*, 1995). The length and composition of the transmembrane domain (TMD) correlates well with the physiological steady-state distributions of these proteins (Sharpe *et al.*, 2010). For some SNAREs, features of the TMD also appear to play a role in the degradation of rogue proteins that have breached their normal localization boundaries (Valdez-Taubas and Pelham, 2005). Furthermore, in vitro assays that use SNARE-mediated liposome fusion have established the compositional requirements that define both the arrangement of vesicle SNAREs (v-SNAREs) and target SNAREs (t-SNAREs). In all cases, there is an obligate requirement for a transmembrane domain on the v-SNARE (Fukuda *et al.*, 2000; McNew *et al.*, 2000a,b; Parlati *et al.*, 2000). Such in vitro assays have been interpreted as defining the functional v- and t-SNAREs in cells, and this is particularly so for the SNAREs that function in ER–Golgi transport in budding yeast cells. Genetic studies also suggest a minimum number of SNARE complexes functioning in ER–Golgi trafficking (Tsui *et al.*, 2001). Finally, ER–Golgi SNAREs have been shown to cycle between the Golgi and the ER in a COPI-dependent manner, which would presumably require SNAREs to be integrally associated with membranes via their TMDs (Ballensiefen *et al.*, 1998). Thus the TMDS of SNAREs have at least three crucial roles: mediating ER insertion of the de novo–synthesized proteins, directing localization of SNAREs within the endomembrane network, and mediating membrane fusion. The importance of the SNARE TMD is reflected in its robust evolutionary conservation.

RESULTS AND DISCUSSION

During the course of generating site-direct mutants in the ER/Golgi–localized SNARE *BET1*, we discovered that cells expressing Bet1p without a TMD (bet1pΔTMD) remained viable. This finding

This article was published online ahead of print in MBoC in Press (http://www.molbiolcell.org/cgi/doi/10.1091/mbc.E16-05-0277) on July 6, 2016.

*Address correspondence to: David K. Banfield (bodkb@ust.hk).

D.K.B. conceived the project, analyzed data, and wrote the article. C.L. and M.S.Y.L. conducted experiments. C.L. prepared the figures and tables.

Abbreviations used: ALP, alkaline phosphatase; CPY, carboxypeptidase Y; ER, endoplasmic reticulum; GFP, green fluorescent protein; GNS, GFP-Nyv1-Snc1; GPI, glycosylphosphatidylinositol; SNARE, soluble *N*-ethylmaleimide–sensitive fusion attachment protein receptor; TMD, transmembrane domain.

prompted us to examine whether TMDs might also be dispensable for other SNAREs involved in ER–Golgi traffic. To this end, we established a simple assay by which haploid cells in which the single chromosomal copy of the essential candidate SNARE had been deleted were balanced by a counterselectable copy of the wild-type gene on a plasmid (Figure 1A). In two instances in which the candidate SNARE gene was not essential (*SEC22* and *GOS1*), deletion of an additional gene (*GYP1*) rendered these SNAREs essential for growth. This assay was applied to Sed5p (Qa-SNARE) and its SNARE binding partners (Figure 1B).

With the exception of Sed5p and Sec22p (Supplemental Figure S1B), all other SNAREs tested could perform their essential function in the absence of a TMD (Figure 1C). The majority of the viable SNAREΔTMD strains grew robustly at the permissive temperature for yeast cell growth (30°C), whereas *vti1*ΔTMD-, *tlg1*ΔTMD-, and *gos1*ΔTMD-expressing cells were somewhat temperature sensitive (Figure 1C; 37°C). As judged by immunoblotting, four of the six SNAREΔTMDs were expressed at or below wild-type levels, ruling out overexpression as a possible generic explanation for cell survival (Figure 1D and Supplemental Figure S1A). However, previous studies showed that yeast mutants with defects in ER–Golgi transport have an activated unfolded protein response (UPR) and thus upregulate the expression of genes involved in trafficking (Jonikas *et al.*, 2009). To rule out the possibility that activation of the UPR indirectly accounted for the viability of SNAREΔTMD cells, we deleted *IRE1* from cells expressing SNAREΔTMDs. Nevertheless, the inability of yeast cells to activate the UPR did not prevent SNAREΔTMDs from supporting the growth of their corresponding deletion strains (Figure 1E and Supplemental Figure S1B), and thus ER–Golgi SNAREs retain their essential function in the absence of a TMD. We also addressed whether cells remained viable if more than one SNARE lacked a TMD, but this is not the case, at least for *BET1* and *BOS1* (Supplemental Figure S1C). The functional significance of this finding is uncertain, however, as perhaps the simplest explanation is that loss of function reflects a synthetic effect between two hypomorphic mutations.

The most obvious essential role of SNAREΔTMDs would be to function together with their cognate SNARE binding partners as membrane fusogens. Functional SNARE complexes are defined by the so-called 3Q:1R rule, in which three SNAREs (defined as Qa-, b-, and c-) donate an evolutionarily conserved glutamine residue to the zero layer of the SNARE complex, and a single R-SNARE donates an evolutionarily conserved arginine residue (Jahn and Scheller, 2006; Figure 1B). To determine whether a SNAREΔTMD could still function as part of a SNARE complex, we used an in vivo assay that identifies functionally interacting SNAREs (Graf *et al.*, 2005). We chose the only SNARE complex amenable to such an approach, which comprised Sed5p (Qa-SNARE), Bos1p (Qb-SNARE), Bet1p (Qc-SNARE), and Sec22p (R-SNARE). As previously reported, substitution of Bos1p's zero-layer glutamine with an arginine (QR) is lethal to cells, whereas a compensatory substitution in Sec22p at the equivalent position, from an arginine to a glutamine (RQ), restored the 3Q:R ratio and, with it, cell viability (Graf *et al.*, 2005; Figure 1F). Of importance, these observations were recapitulated with *bos1*ΔTMD (Figure 1F), indicating that *bos1*ΔTMD does indeed function as a SNARE.

To explore whether its ΔTMD counterpart retained other well-documented properties of a particular SNARE, we examined genetic interactions. *BET1* could functionally substitute for *SFT1* when present on a high–copy number plasmid (Tsui and Banfield, 2000), and *bet1* ΔTMD could also support the growth of *sft1* Δ cells (Figure 1G). This result is striking because in these cells, a single SNAREΔTMD (bet1p ΔTMD) could replace the function of two otherwise essential v-SNARES—Bet1p and Sft1p (McNew *et al.*, 2000a; Parlati *et al.*, 2000). Additional genetic interactions with SNAREΔTMDs were also conserved, as *bos1*ΔTMD could suppress the temperature sensitivity of *bet1-1* cells (Shim *et al.*, 1991), albeit somewhat less effectively than *BOS1* (Supplemental Figure S1C).

The ability of a SNAREΔTMD to robustly support growth does not necessarily mean that yeast cells expressing such SNAREs are free from any transport defects. We therefore systematically examined the transport of several proteins that traffic from the ER to the Golgi, the vacuole, or the cell surface. We first examined steady-state levels of canonical markers of ER-Golgi transport—the soluble protein carboxypeptidase Y (CPY) and the type I integral membrane protein alkaline phosphatase (ALP). Intermediates in

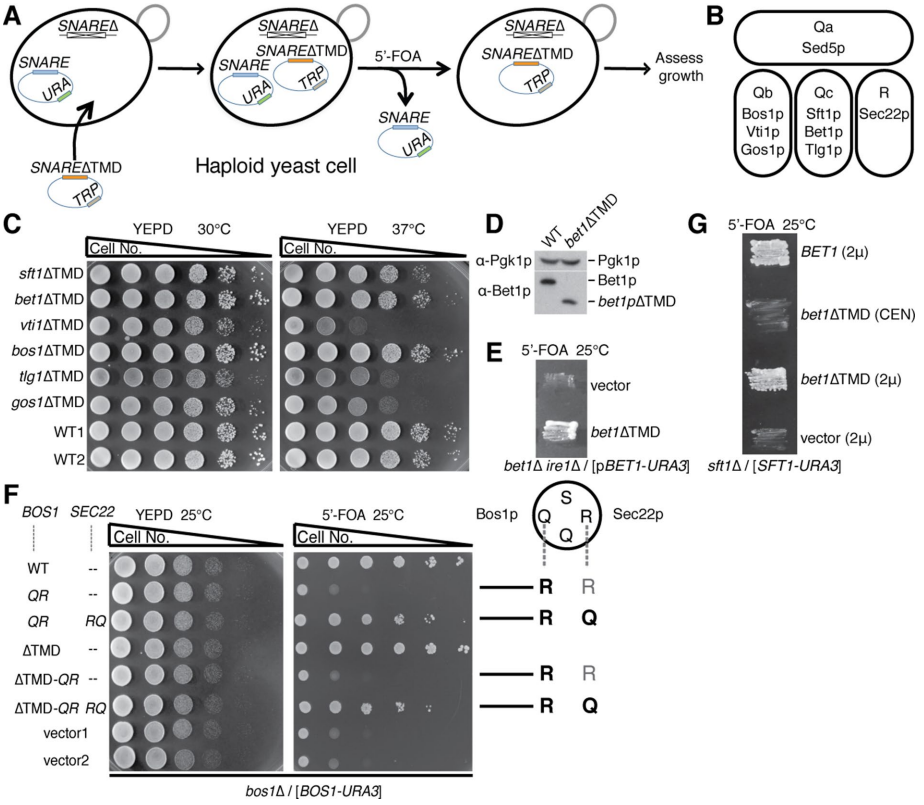

FIGURE 1: ER–Golgi SNAREs lacking their transmembrane domains are functional. (A) Assay used to determine whether SNAREs lacking a transmembrane domain are functional. (B) Sed5p (Qa-SNARE) forms SNARE complexes with a Qb-, a Qc-, and a R-SNARE. (C) Growth profiles of SNARE ΔTMD strains and WT1 (BY4741) and WT2 (SEY6210). (D) Immunostaining of whole-cell extracts from wild-type (BY4741) and *bet1ΔTMD* cells with anti-Bet1p. Pgk1p serves as a gel loading control. (E) Activation of the UPR does not account for the viability of *bet1ΔTMD* cells. (F) bos1pΔTMD functions as a SNARE. (G) Genetic interactions observed with *BET1* are recapitulated with *bet1ΔTMD*.

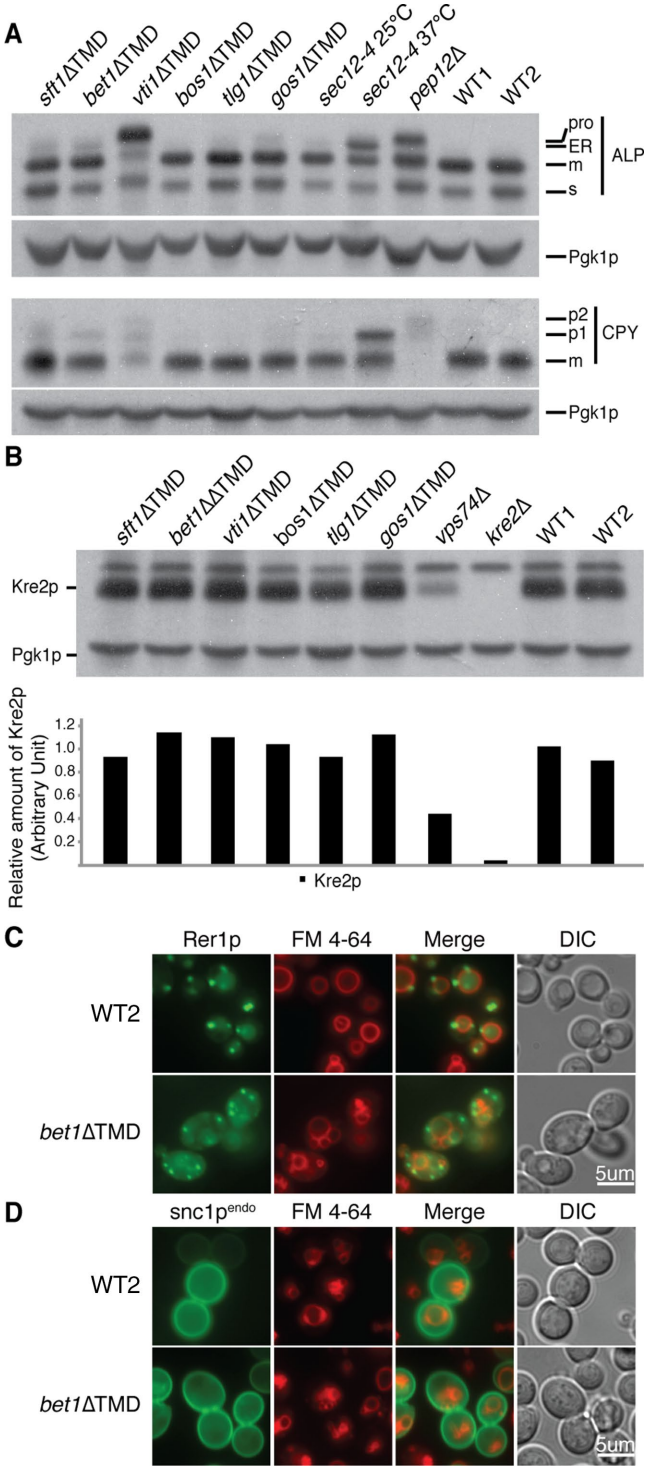

FIGURE 2: SNAREΔTMD strains are not defective in the anterograde transport. (A) WCEs from SNAREΔTMD strains were assayed for defects in the transport and processing of ALP and CPY by immunoblotting with anti-ALP and anti-CPY antibodies. Pgk1p was detected with an anti-Pgk1p antibody, and Pgk1p serves as a gel loading control. For ALP, m and s denote processed forms localized the vacuole, pro denotes ALP that has been delivered to the vacuole but not processed by Pep4p, and ER denotes ALP that is localized to the ER. *sec12-4* cells are deficient ER export at 37°C, and *pep12*Δ cells are deficient in transport from the Golgi to the prevacuolar endosomal compartment. (B) WCEs from SNAREΔTMD strains were treated with endoglycosidase H and then assayed for defects in the retention of the mannosyltransferase Kre2p in the Golgi. *vps74*Δ cells are defective in the Golgi retention of Kre2p. Deglycosylated Kre2p was detected with an anti-Kre2p antibody. Pgk1p serves as a gel loading control. (C) *bet1*Δ*TMD* cells are not defective in the Golgi retention of multispanning membrane protein Rer1p. WT1, SEY6210; WT2, BY4741; see Table 1. (D) *bet1*Δ*TMD* cells are not defective in delivery of snc1p^{endo} from the Golgi to the cell surface. FM4-64 was used to visualize vacuoles.

the transport of CPY and ALP are readily visualized by immunoblotting (Figure 2A). In the majority of the SNAREΔTMD strains, a modest amount of the ER precursor form of ALP could be seen, and in all cases, the Pep4p-dependent cleavage products of ALP were evident and comparable to levels detected in wild-type cells (Figure 2A). Only *vti1*ΔTMD cells showed a substantial defect in the Pep4p-dependent processing of ALP (pro ALP; Figure 2A). Comparable results were obtained upon examination of CPY in SNAREΔTMD-expressing cells. At steady state, only trace amounts of the ER form of CPY were evident, except in the case of *vti1*ΔTMD cells, in which there was a comparatively significant reduction in the amount of mCPY. This result suggests that the bulk of CPY was mislocalized and secreted from cells and indicates that *vti1*ΔTMD cells are not defective in exocytosis (Figure 2A). Nonetheless, the transport and processing of CPY and ALP to the vacuole was not completely blocked in *vti1*ΔTMD cells, as the vacuolar forms of both proteins are clearly evident (Figure 2A). Thus *vti1*ΔTMD cells are not entirely deficient in anterograde transport to the prevacuolar endosome (CPY) or to the vacuole (ALP), and the remaining SNAREΔTMD cells were essentially indistinguishable from wild-type cells.

We next sought to establish whether SNAREΔTMD cells displayed any deficiencies in the transport or retention of membrane proteins in the Golgi. To assess this, we examined the steady-state levels of the Golgi-localized mannosyl transferase Kre2p. Kre2p requires Vps74p for its retention in the Golgi, and cells lacking *VPS74* mislocalize Kre2p to the vacuole, where it is degraded (Schmitz *et al.*, 2008; Tu *et al.*, 2008). The *vps74*Δ cells retained ~40% of wild-type levels of Kre2p, whereas the SNAREΔTMD strains retained 90–100% (Figure 2B). We therefore concluded that SNAREΔTMD cells do not show a significant defect in the Golgi retention of the type II membrane protein Kre2p. Similarly, the distribution of the Golgi-localized multispanning membrane protein Rer1p (Sato *et al.*, 2001) was largely unaffected in SNAREΔTMD cells (Figure 2C and Supplemental Figure S2A). Thus SNAREΔTMD cells are not deficient in COPI-mediated Golgi retention of Rer1p or Kre2p (Tu *et al.*, 2012).

To ascertain whether SNAREΔTMD cells were defective in the exocytic pathway from the Golgi, we examined the transport of an endocytosis-defective variant of the exocytic SNARE Snc1p (hereafter termed snc1p^{endo}; Lewis *et al.*, 2000). In wild-type cells, snc1p^{endo} transits the ER and Golgi before being sorted into exocytic transport vesicles that deposit snc1p^{endo} into the limiting membrane of the cell. In all SNAREΔTMD cells, the transport of snc1p^{endo} to the cell surface was indistinguishable from that of wild-type cells (Figure 2D and Supplemental Figure S2B), and we therefore concluded that SNAREΔTMD cells were not deficient in the exocytic transport of snc1p^{endo}.

Thus far, our data indicate that SNAREΔTMD cells were not defective in anterograde transport or in the retention of Golgi-resident membrane proteins (Figure 2 and Supplemental Figure S4). How, then, can the extent of the transport defects observed for CPY and ALP in *vti1*ΔTMD cells be accounted for? In one scenario, we posit that these phenotypes are epistatic to an anterograde defect in ER–Golgi transport. After fusion of anterograde vesicles with the Golgi,

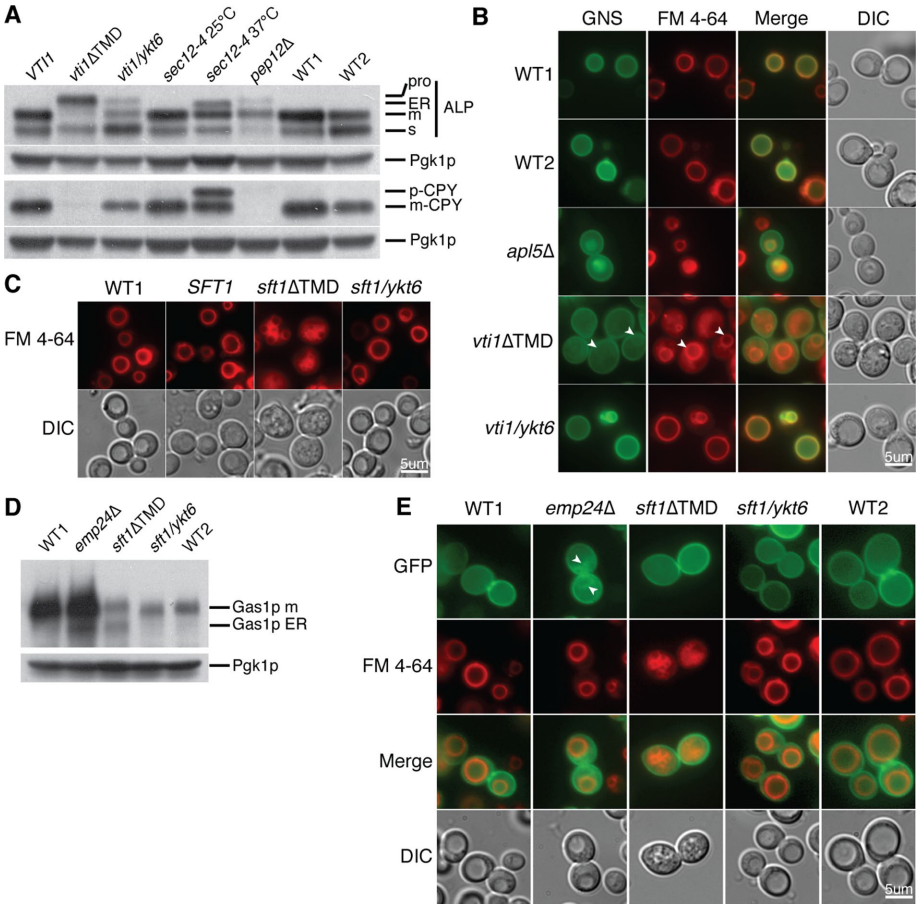

FIGURE 3: Lipid-anchored SNAREs restore transport defects apparent with SNAREΔTMDs. (A) The lipidated form of vti1p (vti1/ykt6) supports the transport and processing of ALP and CPY. (B) The lipidated form of vti1p (vti1/ykt6) functions in the AP3-dependent transport of GNS to the limiting membrane of the vacuole. *APL5* encodes the δ-adaptin–like subunit of AP3. Arrowheads indicate localization of GNS to the limiting membrane of the vacuole. (C) Cells expressing the lipidated form of sft1p (sft1/ykt6) do not have fragmented vacuoles. FM4-64 is used as marker of the yeast vacuole. (D) Cells expressing the lipidated form of sft1p (sft1/ykt6) are not defective in processing of the GPI (glycosylphosphatidylinositol)-anchored protein Gas1p. EMP24 encodes a p24-family member, deficiencies in which result in a kinetic delay in the ER-export of Gas1p. Here m denotes the mature form of Gas1p, and ER denotes the ER or aberrantly glycosylated form of Gas1p. Pgk1p serves as a gel loading control. (E) *sft1*ΔTMD cells do not display a delay in the export of green fluorescent protein (GFP)-Gas1p from the ER. Arrows indicate the ER/nuclear envelope. WT1, SEY6210; WT2, BY4741; see Table 1.

vti1pΔTMD would dissociate from its cognate *cis*-SNARE complex and be released into the cytoplasm, depleting the membrane-associated pool and effectively blocking Vti1p-dependent transport beyond the Golgi. This scenario is consistent with our observations and would account for both the secretion of CPY and the abnormalities in ALP processing we observed (Figure 2A). However, Vti1p binds to four different Qa-SNAREs and participates in Golgi–vacuole transport, Golgi–prevacuolar endosome transport, Golgi–endosomal transport, and, in the cytoplasm, to the vacuole transport pathway (Fischer von Mollard and Stevens, 1999). If all of these anterograde transport steps were simultaneously blocked, we predict that *vti1*ΔTMD cells would display significantly reduced viability (even under standard temperatures for yeast cell growth), be defective in the transport of FM4-64 dye to the vacuole (Vida and Emr, 1995), and have highly fragmented vacuoles, but this is not the case (Figure 1C and Supplemental Figure S2, A and B). We therefore consider it more likely that there is a quantity of vti1pΔTMD that is still available to function in anterograde transport from the Golgi. In fact, *vti1*ΔTMD cells did contain mature forms of both ALP and CPY, consistent with the delivery of these proteins to the vacuole (Figure 2A). The deficiencies in CPY and ALP transport apparent in *vti1*ΔTMD cells would then represent a retrograde trafficking defect brought about by the failure to recycle vti1pΔTMD. Indeed, a failure to recycle the sorting receptor for CPY (Vps10p) could equally well account for the trafficking defects observed in *vti1*ΔTMD cells. In any case, addition of a lipid anchor to vti1p (vti1/ykt6p) restores the trafficking of CPY to the vacuole and substantially improved the transport/processing of ALP (Figure 3A). There is evidence of a retrograde transport route for Vti1p from the vacuole (Bryant *et al.*, 1998), and we speculate that such trafficking is required for the iterative cycles of Golgi–prevacuolar endosomal transport necessary for delivery of hydrolases such as CPY and ALP to the vacuole. Significantly, sorting anomalies in other SNAREΔTMD strains could also be rescued by addition of a lipid anchor, including mislocalization of GNS (GFP-Nyv1-Snc1; see Table 2 in *Materials and Methods*) to the cell surface that occurred in *vti1*ΔTMD cells (Figure 3B), as well as the fragmented vacuolar phenotype and Gas1p transport delays/processing defects observed for *sft1*ΔTMD cells (Figure 3, C–E).

To acquire direct evidence that SNAREΔTMD proteins were deficient in retrograde transport, we examined the recycling of Sec22p and its ΔTMD and lipidated counterparts in *sec12-4* cells. Whole-cell extracts from *sec12-4* cells (expressing Sec22p and sec22pΔTMD or Sec22p and sec22/ykt6p) grown at either the permissive (25°C) or restrictive temperature (37°C) were subjected to successive rounds of centrifugation from which membranes that sediment at 13,000 × *g* (P13, corresponding to the ER) and 100,000 × *g* (P100, corresponding to the Golgi) were collected, solubilized, and analyzed by SDS–PAGE and immunoblotting (Figure 4A). As expected, Sec22p was retrieved from the Golgi in *sec12-4* cells at 37°C, but its subsequent export from the ER was blocked, as evidenced by the absence of Sec22p from the P100 fraction (Figure 4A). By contrast, no equivalent redistribution was observed for sec22pΔTMD, whereas the lipidated form of sec22p (sec22/ykt6p) behaved like wild-type Sec22p (Figure 4A). These results are consistent with Sec22p functioning as a retrograde v-SNARE (Burri *et al.*, 2003) and reveal that Sec22p must be integral to the membrane in order to be recycled from the Golgi to the ER. Comparable findings were obtained using bos1pΔTMD and bos1/ykt6p (Supplemental Figure S3).

We next sought to determine whether sec22pΔTMD and/or its lipidated counterpart (sec22/ykt6p) could form a SNARE complex in cells. Sec22p has been reported to form a SNARE complex with the ER-resident SNAREs Ufe1p, Use1p, and Sec20p in which Sec22p

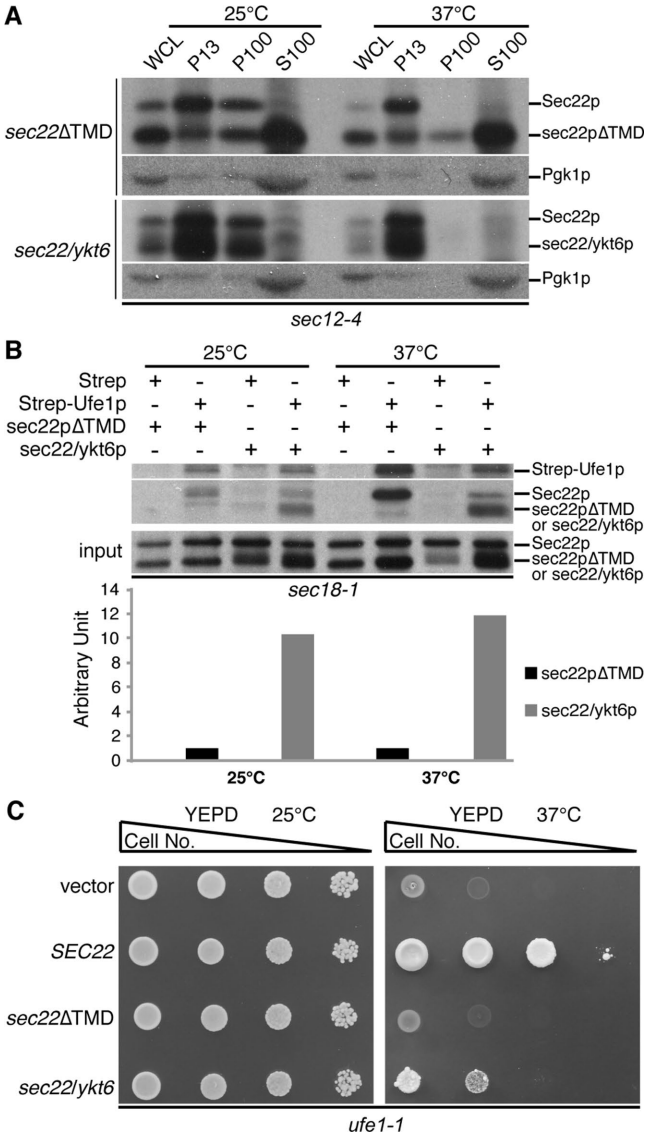

FIGURE 4: sec22pΔTMD cannot be retrieved from the Golgi to the ER by vesicular transport. (A) sec22pΔTMD cannot traffic from the Golgi to the ER. WCL, P13 (membrane pellet 13,000 × *g*), P100 (membrane pellet 100,000 × *g*), and S100 (supernatant 100,000 × *g*). Pgk1p serves as a soluble protein marker of the cytosol. (B) sec22pΔTMD does not form a SNARE complex with Ufe1p. Quantification of the relative amount of sec22pΔTMD and sec22/ykt6p copurified with strep-tagged Ufe1p is presented below. (C) *sec22ΔTMD* does not suppress the temperature-sensitive growth defect of *ufe1-1* cells.

functions as the v-SNARE (Burri *et al.*, 2003). We used yeast cells bearing a temperature-sensitive mutation in *SEC18* (*sec18-1*), which are conditionally defective in the dissociation of trans-SNARE complexes (Hay and Scheller, 1997). Mutant yeast cells expressing Strep-tagged Ufe1p (Strep-Ufe1p) together with wild-type Sec22p and sec22pΔTMD or wild-type Sec22p and sec22/ykt6p were grown at either the permissive (25°C) or restrictive (37°C) temperature, after which Strep-Ufe1p (and its associated proteins) were identified by affinity purification and immunoblotting (Figure 4B). Both wild-type Sec22p and sec22p/ykt6 could be robustly copurified with Strep-Ufe1p, whereas sec22pΔTMD could not. We therefore concluded that only the recycling pool of Sec22p could associate with the ER-localized Ufe1p (Figure 4B). To determine whether sec22/ykt6p was a functional v-SNARE, we took a genetic approach. *SEC22* was previously reported to act as a dosage suppressor of a temperature-sensitive mutation in *UFE1*, which would require retrograde transport of Sec22p from the Golgi to the ER (Figure 4, A–C; Lewis *et al.*, 1997). Consistent with our hypothesis that SNAREΔTMDs are deficient in retrograde transport, we found that *sec22*ΔTMD could not suppress the temperature-sensitive phenotype of *ufe1-1* cells, whereas the *sec22/ykt6* chimera could, albeit less effectively than *SEC22* (Figure 4C).

In sum, our data reveal that the TMD of several ER and Golgi SNAREs, including those that function as v-SNAREs (McNew *et al.*, 2000a; Parlati *et al.*, 2000), are not required for their essential function, anterograde trafficking from the ER or Golgi, or their localization in cells. How can we reconcile our findings with the currently accepted view of how SNAREs are transported in cells and function in membrane fusion? The idea that a newly synthesized SNAREΔTMD might be able to directly associate with its cognate SNAREs on ER membranes may be unlikely, as neither ufe1pΔTMD or use1pΔTMD—two components of the ER t-SNARE—supports the essential function of their corresponding deletion strains (Lewis *et al.*, 1997; Burri *et al.*, 2003; Supplemental Figure S4A). Similarly, the prospect that SNAREΔTMDs are transported from the ER together with their cognate partners is doubtful, as a COPII-binding–deficient form of Sed5p does not affect the incorporation of Bet1p, Bos1p, or Sec22p into ER-derived vesicles (Miller *et al.*, 2005). In addition, the COPII-binding–deficient form of bet1pΔTMD ($L^{51}Q$, $L^{54}Q$ $E^{55}Q$, bet1p-3Q; Mossessova *et al.*, 2003) can still support the growth of *bet1Δ* cells (Supplemental Figure S4B). Thus newly synthesized SNAREΔTMDs may be targeted to and transported from ER via a novel mechanism. Finally, although we did not directly measure membrane fusion, it would appear that, at the very least, a lipidated v-SNARE could mediate fusion in cells (Figure 4). Our observations on the viability and transport characteristics of SNAREΔTMDs are restricted to members of the R-, Qb-, and Qc-SNARE families. Moreover, it appears that the introduction of more than one SNAREΔTMD into cells is not tolerated (Supplemental Figure S1C), although this may be a consequence of a combinatorial reduction of SNAREΔTMDs on the membranes on which they function rather than a reflection of any minimum requirement for cognate SNAREs bearing a TMD.

Why, then, are TMDs of SNAREs evolutionarily conserved? Presumably, for efficient and robust trafficking, cells must reuse components of the transport and fusion machinery rather than rely exclusively on de novo protein synthesis. The conservation of TMDs in SNAREs therefore highlights the importance of retrograde transport pathways in cells and in particular the need to recycle SNAREs.

MATERIALS AND METHODS

Materials

Strep-Tactin beads were purchased from IBA GmbH (Göttingen, Germany). Protease inhibitors (EDTA-free complete protease inhibitor cocktail, Pefabloc SC [4-(2-aminoethyl) benzenesulfonyl fluoride hydrochloride]) and endoglycosidase H were purchased from Roche (Mannheim, Germany). The anti-Pgk1p antibody was purchased from Molecular Probes (Eugene, OR). Anti-Kre2p and anti-Sec22p antibodies were from the Banfield Laboratory collection. The anti-Gas1p antibody was kindly provided by Howard Riezman (University of Geneva, Geneva, Switzerland). The anti–Strep tag antibody was purchased from Qiagen (Chatsworth, CA). Anti-rabbit immunoglobulin G (IgG) horseradish peroxidase (HRP) antibody, anti-mouse IgG HRP–conjugated antibody, and concanavalin A were all purchased from Sigma-Aldrich (Poole, UK).

All SNAREΔTMD and chimera strains were derived from SEY6210 or BY4741 wild-type strains, except *vti1*ΔTMD, which was derived by sporulation and tetrad dissection from a SEY6210/BY4741 diploid strain. Table 1 lists the yeast strains and Table 2 the plasmids used in this study.

Methods

Yeast manipulation and plasmid counterselection assay. Plasmids were transformed into mid log-phase yeast culture using lithium acetate/single-stranded carrier DNA/polyethylene glycol method (Gietz and Woods, 2002). For the plasmid counterselection assay, cells were patch onto minimal medium with full amino acid complement and 5-fluoroorotic acid (5-FOA; Invitrogen, Carlsbad, CA) at 1 mg/ml. A repatch on 5-FOA medium was carried out after 2 d to ensure complete loss of *URA3*-bearing plasmid.

Microscopy. Yeast transformants were transferred into selective minimal medium and grown overnight at 25°C. Overnight cultures were diluted to an OD_{660} of ~0.2 into new selective minimal medium or yeast extract/peptone/dextrose and shaken for 3 h at

	Genotype	Source
SEY6210	*MATα leu2-1, 112 ura3-52 his3Δ200 trp1Δ901 suc2Δ9*	Lab collection
BY4741	*MATα his3Δ1* leu2Δ0 *met15Δ0 ura3Δ0*	Lab collection
SARY160	*MATα leu2-1, 112 ura3-52 his3Δ200 trp1Δ901 suc2Δ9 sft1::LEU2*, p*SFT1*[2μ *URA3* P_{TPI1} *SFT1*]	Lab collection
SARY1347	*MATα leu2-1, 112 ura3-52 his3Δ200 trp1Δ901 suc2Δ9 sft1::LEU2*, p*sft1ΔTMD*[*CEN TRP1 sft1ΔTMD*]	This study
SARY1940	*MATα leu2-1, 112 ura3-52 his3Δ200 trp1Δ901 suc2Δ9 sft1::LEU2*, p*sft1/ykt6* [*CEN TRP1 sft1/ykt6*]	This study
SARY1389	*MATα leu2-1, 112 ura3-52 his3Δ200 trp1Δ901 suc2Δ9 sft1::LEU2*, p*SFT1*[2μ *URA3* P_{TPI1} *SFT1*], *ire1::KanMX*,	This study
SARY260	*MATα his3Δ1* leu2Δ0 *ura3Δ0 bos1::KanMX*, p*BOS1* [2μ *URA3 gBOS1*]	Lab collection
SARY1933	*MATα his3Δ1* leu2Δ0 *ura3Δ0 bos1::KanMX*, p*bos1*ΔTMD [*CEN LEU* P_{TPI1} *bos1*ΔTMD]	This study
SARY2618	*MATα his3Δ1* leu2Δ0 *ura3Δ0 bos1::KanMX*, p*BOS1* [2μ *URA3 gBOS1*], *ire1::SpHis5*	This study
SARY270	*MATα, his3Δ1* leu2Δ0 *met15Δ0 ura3Δ0 bet1::KanMX*, p*BET1* [2 μ, *URA3*, *gBET1*]	Lab collection
SARY1895	*MATα, his3Δ1* leu2Δ0 *met15Δ0 ura3Δ0 bet1::KanMX*, p*bet1*ΔTMD [*CEN HIS* P_{TPI1} *bet1*ΔTMD]	This study
SARY4379	*bos1*ΔTMD::*Kl LEU2*, *bet1*::*KanMX*, p*BET1*[2 μ *URA3*, gBET1]	This study
SARY2620	*MATα, his3Δ1* leu2Δ0 *met15Δ0 ura3Δ0 bet1::KanMX*, p*BET1* [2 μ, *URA3*, *gBET1*], *ire1::SpHis5*	This study
SARY298	*MATα his3Δ1* leu2Δ0 *met15Δ0 ura3Δ0* lys2Δ0 *vti1*::*kanMX4*, p*VTI1* [2μ *URA3 gVTI1*]	Lab collection
SARY366	*MATα trp1 vti1::KanMX*	Lab collection
SARY1931	*MATα trp1 vti1::KanMX* p*vti1*ΔTMD [*CEN TRP1* P_{TPI1} *vti1*ΔTMD]	This study
SARY1861	*MATα trp1 vti1::KanMX* p*vti1/ykt6* [*CEN TRP1* P_{VTI1} *vti1/ykt6*]	This study
SARY1944	*MATα his3Δ1* leu2Δ0 *ura3Δ0 tlg1::KanMX*, p*tlg1*ΔTMD [*CEN HIS* P_{TPI1} *tlg1*ΔTMD]	This study
SARY1945	*MATα his3Δ1* leu2Δ0 *ura3Δ0 gyp1::KlLEU2 gos1::KanMX*, p*gos1*ΔTMD [*CEN HIS* P_{TPI1} *gos1*ΔTMD]	This study
SARY580	*MATα his3Δ1 leu2Δ0 met15Δ0 ura3Δ0 pep12::KanMX*	EUROSCARF
RSY263	*MATα ura3 his4 sec12-4*	Lab collection
RSY271	*MATα ura3 his4 sec18-1*	Lab collection
RSY1312	*MATa leu2-3, 112 trp1 ura3-52 sec27-1*	Lab collection
ANY112	*MATα ura3-52 bet1-1*	Lab collection
Y14317	*MATα his3Δ1 leu2Δ0 lys2Δ0 ura3Δ0 kre2::kanMX4*	EUROSCARF
Y01428	*MATα his3Δ1* leu2Δ0 *met15Δ0 ura3Δ0 vps74::kanMX4*	EUROSCARF
Y01097	*MATα his3Δ1* leu2Δ0 *met15Δ0 ura3Δ0 alp5::kanMX4*	EUROSCARF
Y04567	*MATα his3Δ1* leu2Δ0 *met15Δ0 ura3Δ0 emp24::kanMX4*	EUROSCARF
UFE1	*MATα, ura3, ade2, his, trp1, ufe1::TRP1*, balanced with UFE1 in URA3 plasmid	M. Lewis (MRC-LMB, Cambridge, UK)
MLY-101	*MATα, ura3, ade2, his, trp1, ufe1::TRP1* containing p*UT*1 (*ufe1-1*, *LEU2*, CEN)	M. Lewis
SARY1988	*MATα,* sporulated from Y24465 (from Open System YKO library) balanced with pRS416-gUSE1 plasmid	Lab collection
SED5	*MATα, sed5::LEU2*, pRS316-g*SED5*	Lab collection
SARY1313	*MATα, sec22::KanMX, gyp1::Kl LEU2, SEC22-URA3*	Lab collection

EUROSCARF, European *Saccharomyces cerevisiae* Archive for Functional Analysis, Institute for Molecular Biosciences, Johann Wolfgang Goethe-University Frankfurt, Frankfurt, Germany.

TABLE 1: Yeast strain used in this study.

Plasmid	Description	Source
pRS413	CEN, *HIS3*	Lab collection
pSY413TC	pRS413 carrying a 1-kb *TPI1* promoter between *Xho*I and *Hin*dIII sites and a 250–base pair *CYC1* transcription terminator between *Sac*II and *Sac*I sites	This study
pRS415	CEN, *LEU2*	Lab collection
pSY415TC	pRS415 carrying a 1-kb *TPI1* promoter between *Xho*I and *Hin*dIII sites and a 250–base pair *CYC1* transcription terminator between *Sac*II and *Sac*I sites	This study
pRS416	CEN, *URA3*	Lab collection
pSY416TC	pRS416 carrying a 1-kb *TPI1* promoter between *Xho*I and *Hin*dIII sites and a 250–base pair *CYC1* transcription terminator between *Sac*II and *Sac*I sites	This study
pRS424	2μ, *TRP1*	Lab collection
pSY424TC	pRS424 carrying a 1-kb *TPI1* promoter between *Xho*I and *Hin*dIII sites and a 250–base pair *CYC1* transcription terminator between *Sac*II and *Sac*I sites	This study
pRS426	2μ, *URA3*	Lab collection
pSY426TC	pRS426 carrying a 1-kb *TPI1* promoter between *Xho*I and *Hin*dIII sites and a 250–base pair *CYC1* transcription terminator between *Sac*II and *Sac*I sites	This study
p*sft1*ΔTMD	*sft1*ΔTMD (amino acids 1–125) coding sequence in pRS414 (*CEN TRP1*)	Lab collection
p*sft1/ykt6*	*sft1/ykt6* (*sft1*ΔTMD linked with coding sequence of last 8 amino acids of Ykt6p) in pRS414 (*CEN TRP1*)	This study
pSY58.2	*vti11*ΔTMD (amino acids 1–189) coding sequence as a *Eco*RI/*Bam*HI fragment in pSY414TC (CEN, *TRP1*)	This study
pSY36.2	*vti1/ykt6* (*vti1*ΔTMD linked with coding sequence of last 8 amino acids of Ykt6p) with *VTI1* promoter in pRS414 (*CEN TRP1*)	This study
pSY16.1	*BOS1* coding sequence with its own promoter in pRS415 (CEN, *LEU2*)	This study
pSY60	*BOS1* coding sequence with its own promoter as an *Xho*I/*Sac*I fragment in pRS426 (2μ, *URA3*)	This study
pSY62	*bos1*ΔTMD (amino acids 1–247) coding sequence as a *Hin*dIII/*Bam*HI fragment in pSY415TC (CEN, *LEU2*)	This study
pSY63	*bos1*ΔTMD coding sequence as a *Hin*dIII/*Bam*HI fragment in pSY426TC (2μ, *URA3*)	This study
pSY211.2	*bos1*ΔTMD coding sequence in pSY416TC (CEN, *URA3*)	This study
pSY20.3	*bos1/ykt6* coding sequence in pSY416TC (CEN, *URA3*)	This study
pSY171.1	*bos1*Q186RΔTMD coding sequence with its own promoter in pRS415 (CEN, *LEU2*)	This study
pSY172.1	*bos1*Q186R coding sequence with its own promoter in pRS415 (CEN, *LEU2*)	This study
pSY178	*sec22*R157Q coding sequence with its own promoter in pRS413 (CEN, *HIS3*)	This study
pSY18	*SEC22* coding sequence with *TPI1* promoter in pRS416 (CEN, *URA3*)	This study
pSY214.1	*sec22*ΔTMD (amino acids 1–184) with *TPI1* promoter in pRS416 (CEN, *URA3*)	This study
pSY174.9	*sec22/ykt6* (*sec22*ΔTMD linked with coding sequence of last 8 amino acids of Ykt6p) with *TPI1* promoter in pRS416 (CEN, *URA3*)	This study
NAT- *sec22*ΔTMD	*sec22*ΔTMD with ClonNAT marker in pRS413TC (CEN, *HIS3*)	This study
NAT-*sec22/ykt6*	*sec22/ykt6* with ClonNAT marker in pRS413TC (CEN, *HIS3*)	This study
pSY198.2	*NStrep-UFE1* with *TPI1* promoter in pRS416 (CEN, *URA3*)	This study
pSY215.1	*BET1* coding sequence as an *Eco*RI/*Bam*HI fragment in pSY416TC (CEN, *URA3*)	This study
pWT81	*gBET1*-pHUC13 from pHUC13 library	Lab collection
pWT125.1	*gBET1* as an *Eco*RI/*Bam*HI fragment in pSY425 (2μ, *LEU2*)	Lab collection
pSY151.1	*bet1-3Q* (L51Q, L54Q, E55Q) coding sequence in pSY425TC (2μ, *LEU2*)	This study
pSY42.3	*bet1*ΔTMD (amino acids 1–123) coding sequence as an *Eco*RI/*Bam*HI fragment in pSY413TC (CEN, *HIS3*)	This study
pSY44.1	*bet1*ΔTMD coding sequence as an *Eco*RI/*Bam*HI fragment in pSY424TC (2μ, *TRP1*)	This study
pSY154.1	*bet1-3Q*-ΔTMD coding sequence in pSY425TC (2μ, *LEU2*)	This study

TABLE 2: Plasmids used in this study.

Continues

Plasmid	Description	Source
pSY75	*tlg1*ΔTMD (amino acids 1–204) coding sequence as an *Eco*RI/*Bam*HI fragment in pSY413TC (CEN, *HIS3*)	This study
pSY76	*gos1*ΔTMD (amino acids 1–203) coding sequence as an *Eco*RI/*Bam*HI fragment in pSY413TC (CEN, *HIS3*)	This study
pSY95.2	*gUSE1* in pRS425 ((2μ, *LEU2*)	This study
pSY97.2	*use1*ΔTMD in pSY413TC (CEN, *HIS3*)	This study
pSY96.3	*UFE1* coding sequence in pSY413TC (CEN, *HIS3*)	This study
pSY94.1	*ufe1*ΔTMD in pSY413TC (CEN, *HIS3*)	This study
GFP-Rer1p	*RER1* coding sequence with 3′ untranslated region as a *Mfe*I/*Bam*HI fragment behind sequences expressing GFP controlled by *TPI1* promoter in pRS416 (CEN, *URA3*)	Lab collection
GFP-snc1^{endo}	Valine 40 and methionine 43 of Snc1p were both substituted to alanine; GFP was linked to the N-terminal of this mutant, controlled by *TPI1* promoter in pRS416 (CEN, *URA3*)	Lab collection
pGNS	Coding sequence of TMD of GFP-Nyv1p was replaced by that of Snc1p, controlled by *TPI1* promoter in pRS416 (CEN, *URA3*)	H. Pelham (MRC-LMB, Cambridge, UK)
pRS414-gSED5	*gSED5* in pRS414 (CEN, TRP1)	Lab collection
pSY52.4	*sed5*ΔTMD (amino acids 1–319) coding sequence as an *Eco*RI/*Bam*HI fragment in pSY424TC (2μ, TRP1)	This study
pGAS1-GFP	Coding sequence of GAS1-GFP in pRS416 (CEN, *URA3*)	Laura Popolo (University of Milan, Italy)

TABLE 2: Plasmids used in this study. Continued

25°C. For experiments involving 37°C temperature incubations, cultures were incubated in shaking water bath (at 37°C) and transferred to an ice-chilled water bath immediately after incubation. Cell suspensions in sterile water were placed onto glass slides precoated with 1 mg/ml concanavalin A. Coverslips were then applied and sealed with nail polish. Cells were immediately examined using a Zeiss Axioskop (Carl Zeiss, Jena, Germany). Images were obtained using a Spot RT3 monochrome digital camera (Diagnostic Instruments, Sterling Heights, MI) and processed using Adobe Photoshop, version 6.

Endoglycosidase H treatment. Endoglycosidase H digestion was carried out according to the procedure described by Tu *et al*. (2008). Cells were cultured at 25°C to mid logarithmic phase (OD_{660} of 0.6–0.8). The cell pellets were incubated with 0.1 M NaOH at room temperature for 5 min. The cells were resuspended in 100 μl of SDS sample buffer containing 1× EDTA-free complete protease inhibitor, 1 mM Pefabloc, and 5 mM dithiothreitol, incubated at 100°C for 5 min, and centrifuged for 1 min at 13,000 rpm. Soluble fractions were supplemented with 5 mU of endoglycosidase H and 80 mM potassium acetate, pH 5.6, after which samples were incubated at 37°C for 2 h. Mock samples were treated and incubated in the same way but without the addition of endoglycosidase H.

Differential centrifugation. Differential centrifugation was performed based on Holthuis *et al*. (1998) with the following modifications. *sec22*ΔTMD- or *sec22/ykt6*-containing *sec12-4* cells were cultured at 25°C to mid logarithmic phase (OD_{660} of 0.6–0.8), or were shifted to 37°C for 1 h after 25°C culturing. Cells were harvested, spheroplasted, and resuspended in 10 mM 4-(2-hydroxyethyl)-1-piperazineethanesulfonic acid, pH 7.5, 12.5% sucrose, and a 1× protease inhibitor cocktail (EDTA-free Complete). The suspension was lysed with Dounce homogenizer by 15 strokes at 4°C. The lysate was centrifuged at 500 × *g* for 10 min at 4°C. The supernatant was collected as whole-cell lysate (WCL). WCL was centrifuged at 13,000 × *g* for 10 min, and the supernatant was collected as P13 (ER, plasma membrane, and vacuole fractions). P13 was subjected to centrifugation at 100,000 × *g* for 1 h at 4°C in a TLS55 rotor (Beckman, Brea, CA) to separate the P100 (Golgi, endosome, and small vesicle fraction) and S100 (cytoplasm; Lewis and Pelham, 1996; Wooding and Pelham, 1998). Proportional amounts of the WCL, P13, P100, and S100 were subjected to SDS–PAGE and immunoblotting using anti-Sec22p, anti-Bos1p, and anti-Pgk1p antibodies.

Coprecipitation assay. The *sec18-1* cells were cotransformed with either pSY2114.1 (*sec22*ΔTMD) or pSY174.9 (*sec22/ykt6)* together with pSY198.2 (Strep-Ufe1p; see Table 2). Transformants were grown at 25°C to mid logarithmic phase (OD_{660} of 0.6–0.8) or shifted to 37°C for 1 h after 25°C culture. After spheroblast preparation, the equivalent of 60 OD_{660} cells were lysed in 1 ml of lysis buffer containing 0.1% Triton X-100, 100 mM Tris/HCl, pH 8, 1 mM EDTA, 150 mM NaCl, and a 1× protease inhibitor cocktail. WCL was incubated with 50 μl of Strep-Tactin beads at 4°C for 1 h. After three washes, beads were subjected to SDS–PAGE and immunoblotting using anti-Strep and Sec22p antibodies.

Quantification of immunoblots

Differential centrifugation. After immunoblotting, corrected integrated density measurements (in which background densities were subtracted) were made of relevant bands from x-ray films using ImageJ, version 1.48 (imagej.nih.gov/ij). Data are expressed as ratios (e.g., integrated density of P13/integrated density of P13 + P100) and are represented graphically below the immunoblot image (Supplemental Figure S3).

Coprecipitation. After immunoblotting, corrected integrated density measurements (in which the background densities were subtracted) were made of relevant bands from x-ray films using ImageJ, version 1.48. Data were generated and plotted as follows. At each of the two temperatures, the ratio of the corrected integrated density of *sec22*ΔTMD coprecipitated with the corrected integrated density of Strep-Ufe1p (*sec22*ΔTMD/Strep-Ufe1p) was arbitrarily set to 1. The equivalent values for sec22p/ykt6/Strep-Ufe1p were then determined based on the data from *sec22*ΔTMD/ Strep-Ufe1p. Thus, at 25°C, ~10-fold more sec22p/ykt6 coprecipitated with Strep-Ufe1p than did *sec22*ΔTMD (Figure 4, B and C).

ACKNOWLEDGMENTS

We thank Mike Lewis and Laura Popolo for providing strains and plasmids and Yusong Guo, Hyokeun Park, and Linna Tu for critiquing the manuscript. D.K.B. acknowledges the contributions of Marco M.K. Tsui and Wai Ming Li in the initial stages of this work. This work was supported by grants from the Research Grants Council of Hong, 66009, 660011, and 660013 to D.K.B., as well as by HKUST10/CRF/12R and AoE/M-05/12. D.K.B. was a Croucher Foundation Senior Research Fellow.

REFERENCES

Ballensiefen W, Ossipov D, Schmitt HD (1998). Recycling of the yeast v-SNARE Sec22p involves COPI-proteins and the ER transmembrane proteins Ufe1p and Sec20p. J Cell Sci 111(Pt. 11), 1507–1520.

Bryant NJ, Piper RC, Weisman LS, Stevens TH (1998). Retrograde traffic out of the yeast vacuole to the TGN occurs via the prevacuolar/endosomal compartment. J Cell Biol 142, 651–663.

Burri L, Varlamov O, Doege CA, Hofmann K, Beilharz T, Rothman JE, Sollner TH, Lithgow T (2003). A SNARE required for retrograde transport to the endoplasmic reticulum. Proc Natl Acad Sci USA 100, 9873–9877.

Chen YA, Scheller RH (2001). SNARE-mediated membrane fusion. Nat Rev Mol Cell Biol 2, 98–106.

Fischer von Mollard G, Stevens TH (1999). The Saccharomyces cerevisiae v-SNARE Vti1p is required for multiple membrane transport pathways to the vacuole. Mol Biol Cell 10, 1719–1732.

Fukuda R, McNew JA, Weber T, Parlati F, Engel T, Nickel W, Rothman JE, Sollner TH (2000). Functional architecture of an intracellular membrane t-SNARE. Nature 407, 198–202.

Gietz RD, Woods RA (2002). Transformation of yeast by lithium acetate/single-stranded carrier DNA/polyethylene glycol method. Methods Enzymol 350, 87–96.

Graf CT, Riedel D, Schmitt HD, Jahn R (2005). Identification of functionally interacting SNAREs by using complementary substitutions in the conserved '0' layer. Mol Biol Cell 16, 2263–2274.

Hay JC, Scheller RH (1997). SNAREs and NSF in targeted membrane fusion. Curr Opin Cell Biol 9, 505–512.

Holthuis JC, Nichols BJ, Pelham HR (1998). The syntaxin Tlg1p mediates trafficking of chitin synthase III to polarized growth sites in yeast. Mol Biol Cell 9, 3383–3397.

Jahn R, Scheller RH (2006). SNAREs–engines for membrane fusion. Nat Rev Mol Cell Biol 9, 631–643.

Jonikas MC, Collins SR, Denic V, Oh E, Quan EM, Schmid V, Weibezahn J, Schwappach B, Walter P, Weissman JS, Schuldiner M (2009). Comprehensive characterization of genes required for protein folding in the endoplasmic reticulum. Science 323, 1693–1697.

Kutay U, Ahnert-Hilger G, Hartmann E, Wiedenmann B, Rapoport TA (1995). Transport route for synaptobrevin via a novel pathway of insertion into the endoplasmic reticulum membrane. EMBO J 14, 217–223.

Lewis MJ, Nichols BJ, Prescianotto-Baschong C, Riezman H, Pelham HR (2000). Specific retrieval of the exocytic SNARE Snc1p from early yeast endosomes. Mol Biol Cell 11, 23–38.

Lewis MJ, Pelham HRB (1996). SNARE-mediated retrograde traffic from the Golgi complex to the endoplasmic reticulum. Cell 85, 205–215.

Lewis MJ, Rayner JC, Pelham HR (1997). A novel SNARE complex implicated in vesicle fusion with the endoplasmic reticulum. EMBO J 16, 3017–3024.

McNew JA, Parlati F, Fukuda R, Johnston RJ, Paz K, Paumet F, Sollner TH, Rothman JE (2000a). Compartmental specificity of cellular membrane fusion encoded in SNARE proteins. Nature 407, 153–159.

McNew JA, Weber T, Parlati F, Johnston RJ, Melia TJ, Sollner TH, Rothman JE (2000b). Close is not enough: SNARE-dependent membrane fusion requires an active mechanism that transduces force to membrane anchors. J Cell Biol 150, 105–117.

Miller EA, Liu Y, Barlowe C, Schekman R (2005). ER-Golgi transport defects are associated with mutations in the Sed5p-binding domain of the COPII coat subunit, Sec24p. Mol Biol Cell 16, 3719–3726.

Mossessova E, Bickford LC, Goldberg J (2003). SNARE selectivity of the COPII coat. Cell 114, 483–495.

Parlati F, McNew JA, Fukuda R, Miller R, Sollner TH, Rothman JE (2000). Topological restriction of SNARE-dependent membrane fusion. Nature 407, 194–198.

Sato K, Sato M, Nakano A (2001). Rer1p, a retrieval receptor for endoplasmic reticulum membrane proteins, is dynamically localized to the Golgi apparatus by coatomer. J Cell Biol 152, 935–944.

Schmitz KR, Liu J, Li S, Setty TG, Wood CS, Burd CG, Ferguson KM (2008). Golgi localization of glycosyltransferases requires a Vps74p oligomer. Dev Cell 14, 523–534.

Sharpe HJ, Stevens TJ, Munro S (2010). A comprehensive comparison of transmembrane domains reveals organelle-specific properties. Cell 142, 158–169.

Shim J, Newman AP, Ferro-Novick S (1991). The BOS1 gene encodes an essential 27-kD putative membrane protein that is required for vesicular transport from the ER to the Golgi complex in yeast. J Cell Biol 113, 55–64.

Tsui MM, Banfield DK (2000). Yeast Golgi SNARE interactions are promiscuous. J Cell Sci 113(Pt 1), 145–152.

Tsui MM, Tai WC, Banfield DK (2001). Selective formation of Sed5p-containing SNARE complexes is mediated by combinatorial binding interactions. Mol Biol Cell 12, 521–538.

Tu L, Chen L, Banfield DK (2012). A conserved N-terminal arginine-motif in GOLPH3-family proteins mediates binding to coatomer. Traffic 13, 1496–1507.

Tu L, Tai WC, Chen L, Banfield DK (2008). Signal-mediated dynamic retention of glycosyltransferases in the Golgi. Science 321, 404–407.

Valdez-Taubas J, Pelham H (2005). Swf1-dependent palmitoylation of the SNARE Tlg1 prevents its ubiquitination and degradation. EMBO J 24, 2524–2532.

Vida TA, Emr SD (1995). A new vital stain for visualizing vacuolar membrane dynamics and endocytosis in yeast. J Cell Biol 128, 779–792.

Wooding S, Pelham HR (1998). The dynamics of golgi protein traffic visualized in living yeast cells. Mol Biol Cell 9, 2667–2680.